

Research Article

Fully-developed Turbulent Pipe Flow with Heat Transfer Using a Zero-equation Model

Khalid Alammam

Mechanical Engineering Department, King Saud University, P.O. Box 800, Riyadh 11421,
Kingdom of Saudi Arabia, Tel.: +96614676650; Fax: +96614676652

Abstract: Aim of this study is to evaluate a zero-equation turbulence model for fully-developed turbulent pipe flow with heat transfer. Uncertainty is approximated through grid-independence and model validation. Results for mean axial velocity, Reynolds stress and temperature had maximum error of 5%, while results for the friction factor and Nusselt number had negligible error. Both the mean axial velocity and normalized temperature profiles were shown to increase and extend farther in the outer layer with increasing Reynolds number, up to 10^6 . The new turbulence model is equally applicable to developing and external flows using the same constant. For wall-bounded flows, the constant is a function of wall roughness.

Keywords: Heat transfer, nusselt number, reynolds stress, skin friction, turbulence

INTRODUCTION

The problem of turbulence dates back to the efforts of Claude-Louis Navier and George Gabriel Stokes, as well as others in the early nineteenth century. Searching for its solution, it was a source of great despair for many notably great scientists, including Werner Heisenberg, Horace Lamb and many others. The complete description of turbulence remains one of the unsolved problems in modern physics. A great deal of early work on turbulence can be found, for example, in Hinze (1975).

Recently, Direct Numerical Simulation (DNS) has emerged as an indispensable tool to tackle turbulence directly, albeit at relatively low Reynolds numbers. Several DNS studies on turbulent pipe flow have been performed recently, including Eggels *et al.* (1993), Loulou *et al.* (1997) and Wu and Moin (2008). The latter has carried out DNS on a turbulent pipe flow at Reynolds number of 44,000, which is the largest among the other three studies. Mean velocity, Reynolds stresses and turbulent intensities are presented and discussed, along with visualization of flow structure. Good agreement was attained with the Princeton Superpipe data on mean flow statistics and Lawn (1971) data on turbulence intensities. Large Eddy Simulation (LES) is another tool that somewhat bridges between DNS and Reynolds-Averaged Navier-Stokes (RANS) methods. In LES, large turbulent structures in the flow field are resolved, while the effect of Sub-Grid Scales (SGS) are modeled. LES investigation, for example, has been carried out by Rudman and Blackburn (1999) on a turbulent pipe flow at Reynolds number of 38,000. Mean velocity and Reynolds stresses are presented and discussed, along with visualization of

flow structure. Results were reported to compare favorably with measurements.

While much work on isothermal turbulence have been carried out using DNS and LES, less attempts have been carried out to investigate turbulent flow with heat transfer using these methods. For example, Redjem-Saad *et al.* (2007) have investigated fully-developed flow and heat transfer characteristics in pipes using DNS at the low Reynolds number of 5,500 based on bulk velocity and pipe diameter. Main emphasis is placed on Prandtl number effects on turbulent heat transfer. Temperature fluctuations and heat fluxes were found to increase when increasing Pr. The turbulent Prandtl number was found to be independent of Pr for Prandtl number >0.2 . They also confirm the intermittent behavior close to the wall, which is more pronounced with increasing Pr. The predicted Nusselt number is in good agreement with published data. Similar investigation was carried out by Satake *et al.* (2000) who performed DNS analysis on a turbulent pipe flow with heat transfer for five Reynolds numbers, ranging from 5,300 to 40,000 based on the bulk velocity and pipe diameter. Their results of average friction and Nusselt number were in good agreement with published data.

While DNS and LES are fairly accurate for modeling turbulent flows with heat transfer, they remain limited to relatively low-range Reynolds numbers. This drawback explains the wide-spread of turbulence modeling in industrial applications where the use of DNS techniques remains formidable. Turbulence modeling includes eddy viscosity models which utilize the Boussinesq hypothesis, Hinze (1975), for relating the Reynolds stresses to the average flow field. In turn, the eddy viscosity is determined by using

any of a variety of techniques, including zero-, one- and two-equation models, most notably the k-ε model. While such models vary in complexity, they share several shortcomings, including isotropy of the eddy viscosity and the lack of generality in wall treatment. Such shortcomings lead to poor results in separated flows and other non-equilibrium turbulent boundary layers (Yamamoto *et al.*, 2008).

A second-order turbulence model, which also falls under RANS methods, is the Reynolds stress model. While the model relaxes the isotropic assumption, it remains more complicated and costly due to the need for solving six additional transport equations along with many unknown terms. For more on the subject of turbulence modeling, the reader is referred to, for example, Launder and Spalding (1972).

In this study, the accuracy of a zero-equation turbulence model applied to fully-developed pipe flow with constant heat flux at the wall is assessed. Unlike typical eddy-viscosity models, the proposed model does not require the solution of additional transport equations; it allows for an-isotropic eddy-viscosity and requires one constant which is strictly a function of wall roughness. Moreover, the model does not require a wall function because the momentum and energy equations are integrated throughout the flow field. The new model is equally applicable to external flows. For simplicity, steady, axisymmetric and fully-developed pipe flow with constant wall heat flux is considered.

METHODOLOGY

Theory: Starting with the incompressible Navier-Stokes and energy equations in Cartesian index notation and with Reynolds decomposition, averaging and following Boussinesq hypothesis, Hinze (1975), we have:

$$\frac{\partial(\bar{u}_i)}{\partial x_i} = 0 \tag{1}$$

$$\rho \left[\frac{\partial(\bar{u}_i)}{\partial t} + (\bar{u}_j) \frac{\partial(\bar{u}_i)}{\partial x_j} \right] = -\frac{\partial(\bar{p})}{\partial x_i} + \frac{\partial}{\partial x_j} (\mu + \mu_t) \left(\frac{\partial \bar{u}_i}{\partial x_j} + \frac{\partial \bar{u}_j}{\partial x_i} \right) \tag{2}$$

$$\rho c \left[\frac{\partial \bar{T}}{\partial t} + (\bar{u}_j) \frac{\partial \bar{T}}{\partial x_j} \right] = \frac{\partial}{\partial x_j} \left(k + \frac{c\mu_t}{Pr_t} \right) \frac{\partial \bar{T}}{\partial x_j} \tag{3}$$

For simplicity, the normal stresses (except for the thermodynamic pressure), body forces and viscous heating are neglected. $Pr_t = 0.87$, Redjem-Saad *et al.* (2007) and $\mu_t = C Re_t \mu$ is the eddy viscosity, Alammar (2013). C is a non-dimensional function of the wall roughness. For a smooth wall, it is a constant. For isotropic roughness, it is a different constant. $Re_t = |\bar{u}_i| \rho d / \mu$ and d is the distance to the wall. C , therefore, takes the value of that location at the wall. When Eq. (2) is normalized, the shear stresses result in the following:

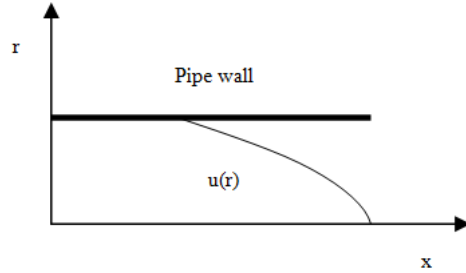


Fig. 1: Schematic of the pipe with fully-developed flow

$$\frac{\partial}{\partial x_j} \left[Re^{-1} + C \frac{|\bar{u}_i| d}{UD} \right] \left(\frac{\partial \bar{u}_i}{\partial x_j} + \frac{\partial \bar{u}_j}{\partial x_i} \right) \tag{4}$$

The second term in the brackets is a non-dimensional number attributed to turbulence. Clearly, this term dominates at high Reynolds numbers. In absence of walls, one plausible length scale would be the mean free path. This would give rise to second-order effects that would be negligible in presence of walls.

Using cylindrical coordinates, Fig. 1 and assuming steady, axisymmetric and fully-developed pipe flow, we have for the momentum equation (after integration once with respect to r):

$$(\mu + \mu_t) \frac{du}{dr} = \frac{r}{2} \frac{dP}{dx} \tag{5}$$

The constant of integration vanishes due to symmetry condition at the center point. The eddy viscosity is given by:

$$\mu_t = b \rho u d \tag{6}$$

where, $b = 0.016$, d is the distance from the wall and the pressure gradient is constant.

With the above assumptions, the radial energy equation becomes:

$$\rho c u \frac{\partial T}{\partial x} = \frac{1}{r} \frac{\partial}{\partial r} \left[r \left(k + \frac{c\mu_t}{Pr_t} \right) \frac{\partial T}{\partial r} \right] \tag{7}$$

where,

$$\frac{\partial T}{\partial x} = \frac{4q}{DU \rho c}$$

Kakac and Yener (1995).

Numerical procedure and uncertainty analysis: There are mainly two sources of uncertainty in Computational Fluid Dynamics (CFD), namely modeling and numerical, Stern *et al.* (1999). Modeling uncertainty can be approximated through theoretical or experimental validation while numerical uncertainty

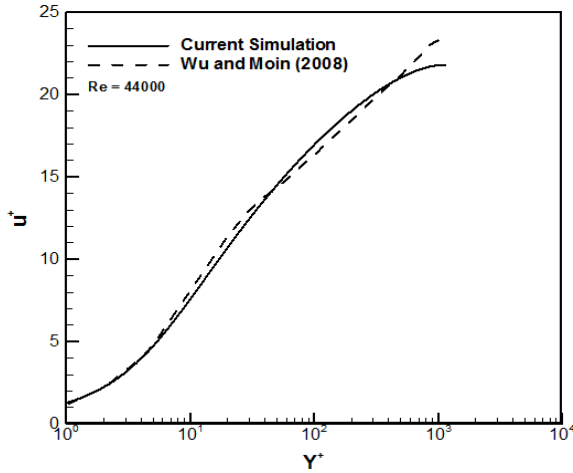


Fig. 2: Mean axial velocity profiles for Re = 44,000

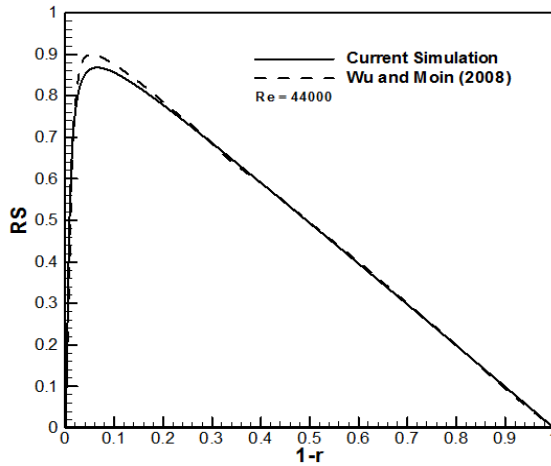


Fig. 3: Reynolds stress profiles for Re = 44,000

can be approximated through grid independence. Numerical uncertainty has two main sources, namely truncation and round-off errors. Higher order schemes have less truncation error. In explicit schemes, round-off error increases with increasing iterations and is reduced by increasing significant digits (machine precision).

Equation (4) and (7) were solved using the Euler second-order algorithm with the no-slip, constant heat flux at the wall and symmetry boundary condition at the center. The fully-developed mean axial velocity is depicted in Fig. 2 for Reynolds number of 44,000, along with DNS results of Wu and Moin (2008). The discrepancy is less than $\pm 5\%$. Such discrepancy could be attributed, in part, to transitional effects in the buffer layer. At the center of the pipe, the discrepancy could be attributed to the enforcement of symmetry condition. The Reynolds stress is shown in Fig. 3 for Reynolds number of 44,000. Again, good agreement is attained between the current simulation and the DNS results, with the discrepancy restricted within the buffer layer and is less than $\pm 5\%$.

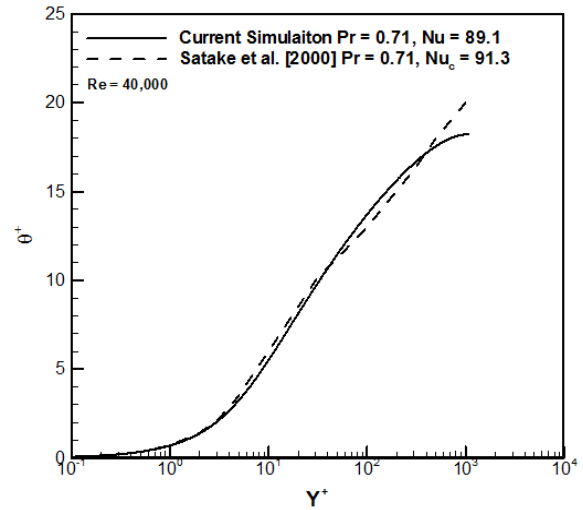


Fig. 4: The normalized temperature profiles for Re = 40,000

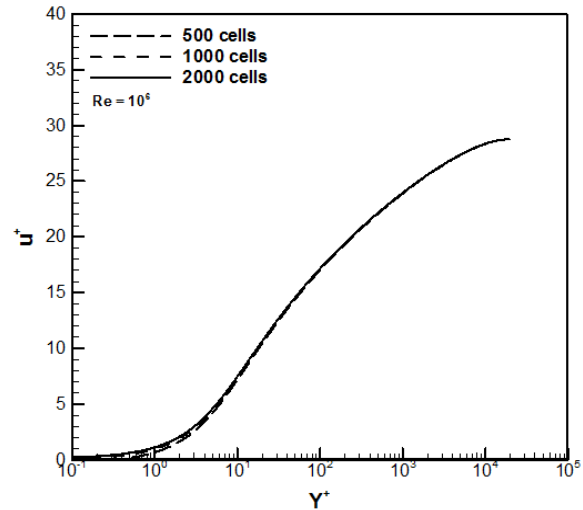


Fig. 5: Mean axial velocity profiles for Re = 10^6

The normalized temperature profile is depicted in Fig. 4 for Reynolds number of 40,000, along with DNS results of Satake *et al.* (2000). The discrepancy is less than $\pm 5\%$. Again, such discrepancy could be attributed, in part, to transitional effects in the buffer layer. At the center of the pipe, the discrepancy could be attributed to the enforcement of symmetry condition.

A grid-independence test is depicted in Fig. 5 for three different, non-uniform cell sizes, namely 500, 1000 and 2000. The error in u^+ is mostly in the laminar sub-layer and is shown to be negligible with 2000 cells for Reynolds number of 10^6 . Hence, we can conclude that the overall uncertainty in the current numerical results is $\pm 5\%$.

RESULTS AND DISCUSSION

The fully-developed mean axial velocity is depicted in Fig. 6 for various Reynolds numbers up to

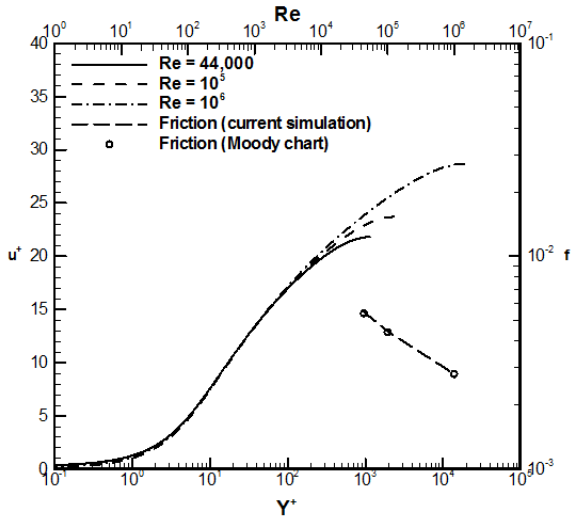


Fig. 6: Mean axial velocity profiles and friction factor for various Reynolds numbers

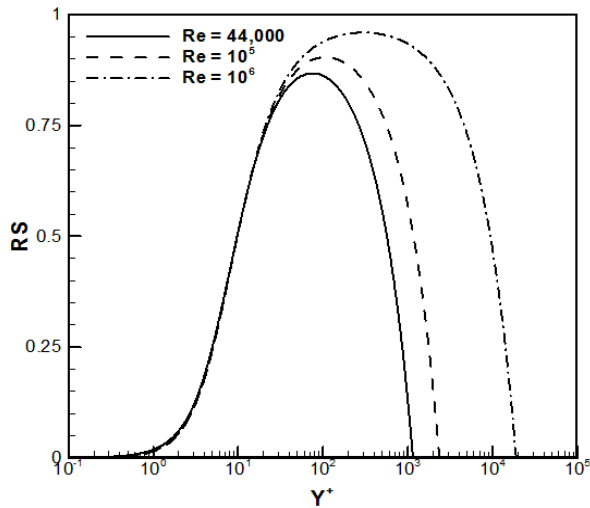


Fig. 7: Reynolds stress profiles for various Reynolds numbers

10^6 . The mean velocity is shown to increase and extend farther in the outer layer with increasing Reynolds number. This is in agreement with published measurements, e.g., Laufer (1954). There is no effect of Reynolds number on the mean velocity below wall distance of 100. The friction factor is also shown in Fig. 5 and compared with data from Moody (1944). The agreement is excellent.

The Reynolds stress is depicted in Fig. 7 for various Reynolds numbers up to 10^6 . Similar to the mean velocity, peak of the Reynolds stress is shown to increase and extend farther in the outer layer with increasing Reynolds number. There is no effect of Reynolds number on the profiles below wall distance of 20. This is different from the case of u^+ where the change was negligible below wall distance of 100.

The normalized temperature profiles are depicted in Fig. 8 for various Reynolds numbers up to 10^6 . The

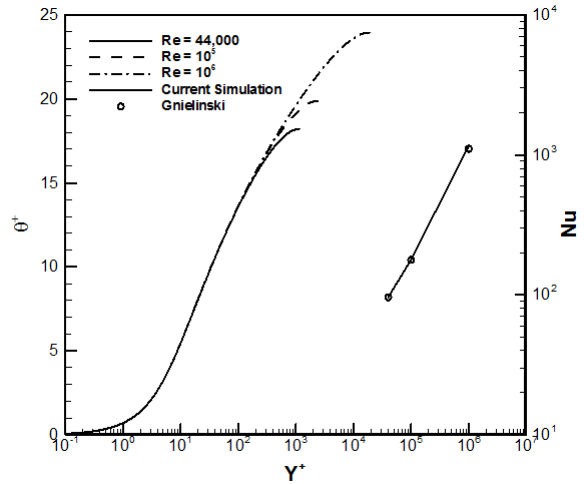


Fig. 8: Normalized temperature profiles and nusselt number for various Reynolds numbers

profiles are shown to increase and extend farther in the outer layer within creasing Reynolds number. There is no effect of Reynolds number on the temperature profiles below wall distance of 100. The Nusselt number is also shown in Fig. 8 and compared with correlation from Gnielinski (1976). The agreement is excellent.

CONCLUSION

Using a zero-equation turbulence model, fully-developed turbulent pipe flow with heat transfer was simulated. Results for the mean axial velocity, Reynolds stress and temperature had maximum error of 5%, while results for the friction factor and Nusselt number had negligible error. Mean axial velocity and temperature profiles were shown to increase and extend farther in the outer layer with increasing Reynolds number. Similar to the mean axial velocity and normalized temperature, peak of the Reynolds stress was shown to increase and extend farther in the outer layer with increasing Reynolds number. The new turbulence model is equally applicable to developing and external flows using the same constant for smooth walls. For wall-bounded flows, the constant is a function of wall roughness.

ACKNOWLEDGMENT

The author would like to extend his sincere appreciation to the Deanship of Scientific Research at King Saud University for its funding of this research through the Research Group Project no RGP-VPP-247.

NOMENCLATURE

- b = A non-dimensional function of wall roughness
- c = Specific heat, J/ (kg K)

D = Pipe diameter, m
 d = Normal distance from the wall, m
 f = Friction factor = $\tau_w/0.5 \rho U^2$
 h = Heat transfer coefficient = $q/(T_w - T_b)$, (W/(m².K))
 k = Thermal Conductivity, (W/mK)
 p = Pressure, Pa
 q = Heat flux through the wall, (W/m²)
 Re = Reynolds number = $U\rho D/\mu$
 Re_t = Non-dimensional parameter = $|\bar{u}_i| \rho d/\mu$
 RS = Reynolds stress = $-\rho \overline{u'v'}/\tau_w$, Pa
 T_b = Bulk temperature = $\frac{R}{0} \int u T r dr / \int_0^R u r dr$, K
 T_τ = Friction temperature = $q/(\rho c U_*)$, K
 T_w = Wall temperature, K
 U = Area-average velocity, m/s
 U* = Friction velocity = $\sqrt{\tau_w/\rho}$, m/s
 \bar{u}_i = Mean velocity component, m/s
 u = Mean axial velocity, m/s
 u⁺ = Normalized mean axial velocity = u/U_*
 x = Axial distance, m
 y⁺ = Non-dimensional wall distance = $rU_*\rho/\mu$
 r = Radial distance, m

Greek symbols:

μ = Fluid dynamic viscosity, N.s/m²
 μ_t = Eddy viscosity, N.s/m²
 ρ = Fluid density, kg/m³
 θ⁺ = $(T_w - T)/T_\tau$
 τ_w = Wall shear stress, Pa

REFERENCES

Alammar, K., 2013. Fully-developed turbulent pipe flow using a zero-equation model. Res. J. Appl. Sci. Eng. Technol., 6(4): 687-690.
 Eggels, J., F. Unger, M. Weiss, J. Westerweel, R. Adrian, R. Friedrich and F. Nieuwstadt, 1993. Fully developed turbulent pipe flow: A comparison between direct numerical simulation and experiment. J. Fluid Mech., 268: 175-209.
 Glielinski, V., 1976. New equations for heat and mass transfer in turbulent pipe and channel flow. Int. Chem. Eng., 16(2): 359-367.
 Hinze, J., 1975. Turbulence. McGraw-Hill Publishing Co., New York.

Kakac, S. and Y. Yener, 1995. Convective Heat Transfer. 2nd Edn., CRC Press, Boca Raton, FL.
 Laufer, J., 1954. The structure of turbulence in fully developed pipe flow. U.S. National Advisory Committee for Aeronautics (NACA), Technical Report 1174.
 Launder, B.E. and D.B. Spalding, 1972. Mathematical Models of Turbulence. Academic Press, NY.
 Lawn, C.J., 1971. The determination of the rate of dissipation in turbulent pipe flow. J. Fluid Mech., 48: 477-505.
 Loulou, P., R. Moser, N. Mansour and B. Cantwell, 1997. Direct simulation of incompressible pipe flow using a b-spline spectral method. NASA-Ames Research Center, Technical Report TM 110436.
 Moody, L.F., 1944. Friction factors for pipe flow. Trans. ASME, 66: 671-684.
 Redjem-Saad, L., M. Ould-Rouiss and G. Lauriat, 2007. Direct numerical simulation of turbulent heat transfer in pipe flows: Effect of Prandtl number. Int. J. Heat Fluid Fl., 28: 847-861.
 Rudman, M. and H. Blackburn, 1999. Large eddy simulation of turbulent pipe flow. Proceeding of the 2nd International Conference on CFD in the Minerals and Process Industry, CSIRO, Melbourne, Australia.
 Satake, S., T. Kunugi and R. Himeno, 2000. High reynolds number computation for turbulent heat transfer in a pipe flow. Proceedings of the 3rd International Symposium on High Performance Computing (ISHPC 2000). LNCS 1940, pp: 514-523.
 Stern, F., R. Wilson, H. Coleman and E. Paterson, 1999. Verification and validation of CFD simulations. IHR Report No. 407, Iowa Institute of Hydraulic Research, College of Engineering, University of Iowa, Iowa City, IA, USA.
 Wu, X. and P. Moin, 2008. A direct numerical simulation study on the mean velocity characteristics in turbulent pipe flow. J. Fluid Mech., 608: 81-112.
 Yamamoto, Y., T. Kunugi, S. Satake and S. Smolentsev, 2008. DNS and k-ε model simulation of MHD turbulent channel flows with heat transfer. Fusion Eng. Des., 83(7-9): 1309-1312.